SOLUTE CONCENTRATION EFFECT ON OSMOTIC REFLECTION COEFFICIENT

ROBERT P. ADAMSKI AND JOHN L. ANDERSON
Department of Chemical Engineering, Carnegie-Mellon University, Pittsburgh, Pennsylvania 15213

ABSTRACT A theory for the effect of concentration on osmotic reflection coefficient, correct to first order, was developed at the molecular level by considering the effect of solute-solute interactions on solute concentration and the fluid stress tensor within a solvent-filled pore. The solvent was modeled as a continuous fluid and potential energies between solute molecules and the pore wall were assumed to be pairwise additive. Although the theory is more general, calculations are presented only for excluded volume effects (hard-sphere for solute, hard-wall for pore). The relationship between the first-order concentration effect and the infinite dilution value of reflection coefficient appears to be geometry independent. The theory is discussed in light of experimental studies of osmotic flow that have recently appeared in the literature.

INTRODUCTION

The reflection coefficient has proven to be a useful parameter with which to quantify the departure of a membrane from semipermeability. In an operational sense it is defined here as

$$\sigma = \frac{-J_v}{L_{p0}\Delta\Pi_\infty}. \tag{1}$$

J_v is the volume flux of solution, or mean flow velocity, through a membrane that separates two reservoirs differing in osmotic pressure by $\Delta\Pi_\infty$. The mechanical pressure is the same in both reservoirs, so that the driving force for the flow derives solely from the osmotic gradient. L_{p0} is the hydraulic coefficient of the membrane that relates the flow rate of pure solvent to an applied mechanical pressure difference. σ equals 1 implies the membrane is semipermeable and hence an osmotic pressure difference has the same effect of generating flow as a mechanical pressure difference of equal magnitude but opposite sign (Mauro, 1960).

There are two basic applications for σ in biological systems. First, it is used to calculate the transmembrane flow given $\Delta\Pi_\infty$; and second, its measured value is often used to infer something about the structure of the membrane, for example, the pore size (e.g., Curry et al., 1976). In the second case a theoretical model relating membrane structure to osmotic flow is required. Nearly all such theories assume infinite dilution of the solute and consider only interactions between one solute molecule and the pore wall. One often used theory is the hydrodynamic pore model that assumes the pores are infinitely long compared with the radius, the pore cross section is geometrically simple, such as a circle or slit, and the solute is a rigid Brownian sphere that views the solvent as a continuum with regard to hydrodynamic effects. There are two methods of deriving the dependence of σ on solute and pore properties. The most common is to model the filtration reflection coefficient ($\sigma^{[f]}$) and then apply Onsager's symmetry theorem to equate $\sigma^{(f)} = \sigma$, as Staverman (1951) first suggested from thermodynamic arguments, and as later supported from a hydrodynamic-thermodynamic analysis by Levitt (1975). A more direct method (Anderson and Malone, 1974) considers the actual mechanism of osmotic flow in terms of pressure distributions generated inside a pore by a gradient in solute concentration. If hydrodynamic effects of the solute molecules are ignored, the direct method gives an expression for σ that is equivalent to that for $\sigma^{(f)}$ for any pore cross section (Anderson, 1981).

One of the experimental problems associated with measuring σ is that osmotic flows are often small. To increase flow rates, relatively large values of $\Delta\Pi_\infty$ are needed, but with macromolecules this means the concentration must be high, i.e., 1–5% by volume. Although Π_∞ can be determined at these concentrations by direct experimentation, and hence corrections for concentration effects on $\Delta\Pi_\infty$ can be made (Massaldi and Borzi, 1982), the possibility that σ itself is concentration dependent is generally ignored. As we shall demonstrate from a theoretical basis, σ depends on solute concentration; thus, the use of infinite dilution models to deduce pore size from a measured value of reflection coefficient could lead to significant error.

In this paper we consider the effect of bulk-phase concentration on the distribution of solute molecules in small pores and the concommitant flows generated by gradients of the concentration. Concentration effects on equilibrium partitioning have been examined in some detail from a basis of statistical mechanics (Glandt, 1980; Anderson and Brannon, 1981), and experimental evidence of a concentration-dependent partition coefficient has been published (for example, Rudin, 1971; Satterfield et al.,

1978; Brannon and Anderson, 1982). The solute-solute forces responsible for the concentration dependence of the distribution also affect hydrostatic stresses within the fluid as a whole (Anderson, 1982). We first summarize the statistical basis of the concentration effect in terms of solute-solute interactions within a small pore and develop the equilibrium stress tensor correct to $0(C_\infty^2)$, where C_∞ is the bulk-phase concentration of solute molecules, for two pore cross-sectional geometries, slit and circular cylinder. The equilibrium stress tensor is then used to derive the velocity field within a pore connecting two bulk solutions of equal mechanical pressure, but unequal solute concentration. By integrating this velocity field over the pore cross section, we compute J_v, and then σ using Eq. 1. The result is of the form

$$\sigma = \sigma_0[1 + \kappa_1 \overline{C}_\infty + 0(C_\infty^2)], \tag{2}$$

where σ_0 is the infinite-dilution reflection coefficient, and $\overline{C}_\infty$ is the arithmetic-mean concentration between the two reservoirs. The parameter, κ_1, is negative for solute molecules whose interactions are predominantly of the hard-sphere type, and depends on the size of the solute molecule relative to that of the pore; our results for the two pore geometries are plotted in Fig. 4. Because the $0(C_\infty^2)$ terms are unknown, Eq. 2 is of limited practical value as written, but can be used to estimate effects at higher solute concentrations by using the reciprocal of the first-order result

$$\sigma \approx \frac{\sigma_0}{1 - \kappa_1 \overline{C}_\infty} \tag{3}$$

The values of κ_1 presented here were calculated assuming hard sphere-hard wall interactions among the solute molecules and the pore wall, but the theory is generally valid for any form of the solute-solute and solute-pore wall potential functions as long as they are pairwise additive. An interesting result is that although κ_1 depends on solute-to-pore dimension and pore geometry, the relationship between κ_1 and σ_0 seems to be geometry independent, as seen in Fig. 6. The consequence of a concentration-dependent reflection coefficient on the interpretation of osmotic flow data in terms of membrane (pore) structure is discussed.

GLOSSARY

a	solute radius, m
b_1	function defined by Eq. 4, m^3
B_2	osmotic virial coefficient (Eq. 26), m^3
C	solute concentration inside pore, m^{-3}
C_∞	solute concentration of bulk solution in equilibrium with pore, m^{-3}
D_n	functions defined by Eq. 37, $m^{3(n-1)}$
$E(\mathbf{x})$	energy of one solute particle whose center is at $\mathbf{x}$, J
F_n	functions defined by Eq. 22c, $m^{3(n-1)}$
G_1, G_1^*	functions defined by Eqs. 23 and 36, m^4
h	$(\delta - y)/a$
h_0	δ/a
$\mathbf{I}$	unit tensor
J_v	solution flux through membrane, m/s
k	Boltzmann constant, $J/°K$
K	partition coefficient for solute between pore and bulk solutions (Eq. 5)
K_0	value of K as $C_\infty \to 0$
ℓ	pore length (membrane thickness), m
L_p	hydraulic coefficient of membrane, $m^3/N \cdot s$
$0(C_\infty^n)$	term proportional to C_∞^n
P_0	solvent pressure, N/m^2
P_∞	total pressure of bulk solution, N/m^2
r	radial position inside circular cylindrical pore, m
r_0	radius of circular cylindrical pore, m
$\bar{r}$	r/r_0
T	temperature, °K;
u_z	osmotic flow velocity in z direction, m/s
$U(r)$	energy of two solute particles separated by center-to-center distance r, J
v	volume of solute molecule, m^3
$\mathbf{x}$	position of center of solute molcule, m
y	position of center of solute molecule, m
$\bar{y}$	y/δ
z	axial position in slit or circular pore, m
α	pore area (volume) fraction in membrane
α_1	coefficient defined by Eq. 6, m^3
δ	half-width of slit pore, m
η,	solution viscosity, $kg/m \cdot s$
η_0	viscosity of solvent, $kg/m \cdot s$
κ_1	coefficient defined by Eq. 2, m^3
λ	a/δ or a/r_0
Π^*	solute stress tensor, N/m^2
Π_∞	osmotic pressure of bulk solution, N/m^2
σ	osmotic reflection coefficient, defined by Eq. 1
σ_0	value of σ as $C_\infty \to 0$
Σ	the part of T contributed by the solute, N/m^2
$\chi^{(p)}$	contribution to Ω from solute-solute forces, N/m^2
Ω	static stress tensor, N/m^2
$\mathbf{T}$	viscous stress tensor, N/m^2.

EQUILIBRIUM CONCENTRATION AND STRESS DISTRIBUTIONS INSIDE SMALL PORES

The pores are assumed to be very long compared with their width, so end effects are negligible. Two cross-sectional geometries are considered, slit and circle, as shown in Fig. 1. The solute molecules are considered spherical particles of radius a that interact directly through a pair of energy $U(r)$, if the particle centers were separated by distance r. The pore wall effect on a particle at position $\mathbf{x}$ is described by the energy $E(\mathbf{x})$. In this section we consider only the equilibrium case, that is, each pore connects two bulk phases that have the same solute concentration C_∞ and mechanical pressure P_∞.

The concentration of solute within a pore, $C(\mathbf{x})$, is not uniform because of the wall interaction. The solute particles distribute themselves in such a way to maintain constant chemical potential equal to the bulk-phase value. The configurational statistics required to compute $C(\mathbf{x})$, given the two interaction energies, U and E, and the bulk solute concentration, C_∞, are described elsewhere (Glandt,

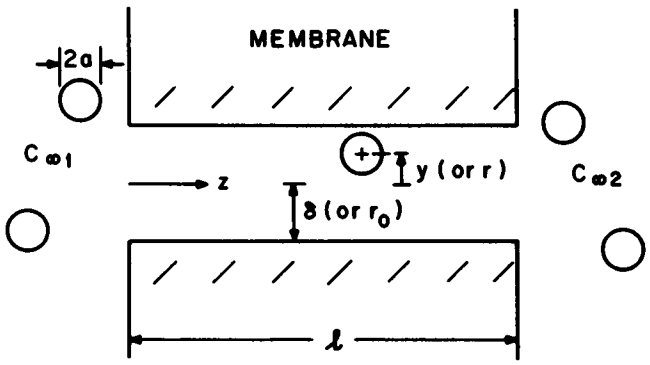

FIGURE 1 Pore geometry. (y, δ) refers to slit cross section, (r, r_0) refers to circle.

1980; Anderson and Brannon, 1981). Truncating the distribution after the $0(C_\infty^2)$ term, the local concentration is given by

$$C = C_\infty \exp(-E(\mathbf{x})/kT)\,[1 + b_1(\mathbf{x})C_\infty], \tag{4}$$

where b_1 is an integral involving E and U over the position of a second solute particle given a first particle at $\mathbf{x}$. In this paper we shall consider only hard sphere-hard wall (HSHW) interactions: U equals ∞, if $r < 2a$; otherwise U equals 0. E equals ∞, if particle center is within distance a of the pore wall; otherwise E equals 0. These interactions describe purely steric effects on the system, that is, two particles cannot overlap and a particle cannot penetrate the pore wall.

In Fig. 2 the solute concentration profile within a slit pore is plotted to illustrate the concentration effect. The dotted line is the result expected if particle-particle interactions are neglected. The effect of these neglected interactions is an excess of solute just outside the excluded region

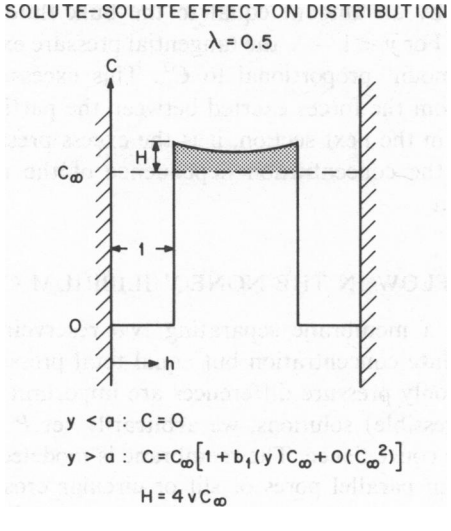

FIGURE 2 Concentration profile within a slit pore, correct to $0(C_\infty^2)$, computed from Eq. 4 and the expression for b_1 in Scheme I. The pair potentials are assumed to be of the HSHW type.

near the pore wall. The partition coefficient, K, is defined as the ratio of mean solute concentration inside the pore to the bulk concentration

$$K \equiv \frac{\langle C \rangle}{C_\infty} = \frac{1}{V_p}\int_{V_p} \frac{C(\mathbf{x})}{C_\infty}\,d\mathbf{x}, \tag{5}$$

where V_p is the pore volume, and $d\mathbf{x}$ the volume differential. From Eq. 4

$$K = K_0[1 + \alpha_1 C_\infty + 0(C_\infty^2)]$$
$$K_0 = \langle \exp(-E/kT) \rangle \tag{6}$$
$$\alpha_1 = K_0^{-1}\langle b_1 \exp(-E/kT) \rangle.$$

The $0(C_\infty^2)$ expression in Eq. 6 means this result neglects terms proportional to C_∞^2 and higher powers. K_0 is the infinite-dilution partition coefficient that was analyzed in some detail by Giddings et al. (1968). α_1 is positive for HSHW interactions because $C > C_\infty$ outside the excluded region near the wall, as shown in Fig. 2. Values for α_1 vs. the ratio of particle-to-pore size (λ) are given by Anderson and Brannon (1981).

Osmotic flows occur because of unbalanced stresses that develop inside pores under nonequilibrium conditions, for example, when the pores connect bulk reservoirs of unequal solute concentration. However, to model these flows we must first appreciate the origin of these stresses under equilibrium conditions. Let Ω be the equilibrium (hydrostatic) stress tensor inside the pore, defined in the usual mechanics sense: $\hat{\mathbf{n}} \cdot \Omega dS$ is the force by solution on the $+n$ side of an element of area dS, where $\hat{\mathbf{n}}$ is the unit normal vector of dS. Even at equilibrium there are variations in Ω because of the existence of the pore wall, which exerts a force, $-\nabla E$, on each solute particle.

From the definition of Ω we write the differential force balance in the pore fluid as

$$\nabla \cdot \Omega - C\nabla E = 0. \tag{7}$$

The stress tensor has two components,

$$\Omega = -P_0\mathbf{I} + \Pi^*, \tag{8}$$

where P_0 is the "solvent pressure" ($\mathbf{I}$ is the unit tensor), and Π^* the solute stress. The latter consists of a kinetic contribution proportional to $C(\mathbf{x})$, and a configurational contribution ($\mathbf{X}^{(p)}$) that accounts for particles exerting forces on each other

$$\Pi^* = -C(\mathbf{x})kT\mathbf{I} + \mathbf{X}^{(p)}(\mathbf{x}). \tag{9}$$

We are using McMillan-Mayer solution theory (Hill, 1960), which assumes that the presence of solvent can be ignored in the configurational statistics of the solute particles, except for its effect on the potentials U and E. Decomposition of the total stress, Ω, into solvent and solute contributions is the mechanical analogue of the McMillan-Mayer thermodynamic model, so that we expect the

following. (*a*) P_0, the solvent pressure, is uniform at equilibrium conditions; and (*b*) the configurational part of the solute stress can be computed from the formula derived by Irving and Kirkwood (1950) for a one component fluid

$$\mathbf{X}^{(p)} = \frac{1}{2}\int_0^1 ds \int \frac{\mathbf{rr}}{r}\frac{dU}{dr}\rho^{(2)}[\mathbf{x} - s\mathbf{r}, \mathbf{x} + (1-s)\mathbf{r}]d\mathbf{r}. \quad (10)$$

In this expression $\mathbf{r}$ is the vector drawn from the center of one particle (located at $\mathbf{x}$) to the center of a second particle (at $\mathbf{x} + \mathbf{r}$), and the integration with respect to the volume differential $d\mathbf{r}$ is over infinite volume. $\rho^{(2)}(\mathbf{x}_1, \mathbf{x}_2)$ is the probability that one particle is at $\mathbf{x}_1$ and a second particle is at $\mathbf{x}_2$. Note that $\rho^{(2)}$ has units of concentration-squared, and hence $\mathbf{X}^{(p)}$ is the sum of particle repulsions, each particle pushing on the other with a force $-dU/dr$.

Before proceeding further, it is worthwhile to examine Ω in bulk solution ($E = 0$). $\rho^{(2)}$ is now only a function of the distance (r) between two particles, so the ds and the angular parts of the dr integrations of $\mathbf{X}^{(p)}$ can be performed directly. Combining Eqs. 8–10 obtains[1]

$$\Omega_\infty = -(P_0 + \Pi_\infty)\mathbf{I} \quad (11a)$$

$$\Pi_\infty = C_\infty kT - \frac{2\pi}{3}\int_0^\infty r^3 \frac{dU}{dr}\rho_\infty^{(2)}(r)dr. \quad (11b)$$

For hard-sphere solute interactions, the above integration is easily performed with the result

$$\Pi_\infty = C_\infty kT(1 + 4vC_\infty) + 0(C_\infty^3), \quad (11c)$$

where v is the volume of one solute particle. In the McMillan-Mayer theory of solutions, Π_∞ is known as the "osmotic pressure" (Hill, 1960). The total pressure of the solution is $P_\infty = P_0 + \Pi_\infty$. Now consider two bulk solutions, designated 1 and 2, that have equal solvent chemical potentials, but different solute concentrations. By the definition of osmotic pressure, the pressure difference, $P_{\infty 2} - P_{\infty 1}$, must equal $\Pi_{\infty 2} - \Pi_{\infty 1}$ to maintain solvent equilibrium; thus, from Eq. 11a we see that $P_{01} = P_{02}$. In general, the solvent pressure is equal among all solutions having the same solvent chemical potential.

Because we are considering only $0(C_\infty^2)$ effects and neglecting higher order contributions, the two-particle distribution function is computed from

$$\rho^{(2)}(\mathbf{x}_1, \mathbf{x}_2) = C_\infty^2 \exp[-U(r_{12})/kT]\exp[-E(\mathbf{x}_1)/kT]\exp[-E(\mathbf{x}_2/kT]. \quad (12)$$

Substitution of this expression into Eq. 10 gives

$$\mathbf{X}^{(p)} = \frac{C_\infty^2}{2}\int_0^1 ds \int_{r\to\infty} \frac{\mathbf{rr}}{r}\frac{dU}{dr}\exp[-U(r)/kT]\exp[-E(\mathbf{x} - s\mathbf{r})/kT]\exp\{-E[\mathbf{x} + (1-s)\mathbf{r}]/kT\}d\mathbf{r}. \quad (13)$$

Because of the wall effect this stress tensor is nonisotropic. For the slit pore geometry, symmetry considerations of Eq. 13 (or, Eq. 10) show

$$\mathbf{X}^{(p)} = X_N^{(p)}(y)\hat{\mathbf{e}}_y\hat{\mathbf{e}}_y + X_T^{(p)}(y)[\mathbf{I} - \hat{\mathbf{e}}_y\hat{\mathbf{e}}_y], \quad (14)$$

where $X_N^{(p)}$ is the stress in the direction perpendicular to the pore wall and $X_T^{(p)}$ acts in the two directions parallel to the wall. In the case of a circular pore cross section,

$$\mathbf{X}^{(p)} = X_{rr}^{(p)}(r)\hat{\mathbf{e}}_r\hat{\mathbf{e}}_r + X_{\phi\phi}^{(p)}(r)\hat{\mathbf{e}}_\phi\hat{\mathbf{e}}_\phi + X_{zz}^{(p)}(r)\hat{\mathbf{e}}_z\hat{\mathbf{e}}_z, \quad (15)$$

where (r, ϕ, z) are circular cylindrical coordinates, z being the axial position along the pore. These scalar components ($X_N^{(p)}$, $X_{rr}^{(p)}$, etc.) are also functions of λ, the ratio of particle size-to-pore size (a/δ for slit, a/r_0 for circle). The values of these components vs. position and λ were computed for HSHW interactions; details of the calculations are given elsewhere (Adamski, 1982). The results for a slit pore are in analytical form, but some numerical integrations were required for the circular pore geometry.

The total equilibrium stress tensor is determined, correct to $0(C_\infty^2)$, by combining Eqs. 8–9 with Eq. 13. The form of Ω is the same as $\mathbf{X}^{(p)}$, either Eq. 14 for slit pores or Eq. 15 for circular pores. The analytical results for the normal and tangential components of Ω in a slit pore are given in Scheme I. In these equations, h is the distance from the pore wall divided by a, and $h_0 = \delta/a$. To illustrate the variation of the equilibrium stress tensor, consider a slit pore when $\lambda = 0.5$. A plot of the "tangential pressure," $-\Omega_T$, is found in Fig. 3. In the region near the wall ($1 > \bar{y} > 1 - \lambda$), where particles are excluded, the pressure equals the solvent pressure, which is uniform

$$-\Omega_T = P_0 = P_\infty - C_\infty kT[1 + 4vC_\infty] = P_\infty - \Pi_\infty. \quad (16)$$

P_∞ is the bulk fluid pressure (outside the pore). Thus, the pressure in the excluded region is lower than the bulk pressure by an amount equal to the bulk fluid osmotic pressure. For $\bar{y} < 1 - \lambda$, the tangential pressure exceeds P_∞ by an amount proportional to C_∞^2. This excess pressure results from the forces exerted between the particles, and as noted in the next section, it is the excess pressure that leads to the concentration dependence of the reflection coefficient.

FLOW IN THE NONEQUILIBRIUM CASE

Consider a membrane separating two reservoirs of different solute concentration but equal total pressure (P_∞). Because only pressure differences are important in liquid (incompressible) solutions, we arbitrarily set $P_\infty = 0$ for algebraic convenience. The membrane is modeled as a set of uniform parallel pores of slit or circular cross section (Fig. 1). Dimensional analysis can be used (Anderson and Malone, 1974) to show that in the limit, $\ell/\delta \to \infty$, there is negligible transport in the lateral (y or r) direction within a pore, and hence the chemical potentials for solute and

[1]Note that Π_∞ is defined such that $\Pi_\infty^* = -\Pi_\infty \mathbf{I}$.

$$\underline{1 < h_0 < 3}$$

$$\text{if } 1 < h < h_0\text{: } b_1 = 4v\left\{1 - \frac{3}{4}(h-1) + \frac{1}{16}(h-1)^3 + \left[1 - \frac{3}{4}(2h_0 - h - 1) + \frac{1}{16}(2h_0 - h - 1)^3\right]H(h - 2h_0 + 3)\right\}$$

(Note: $H[u] = 0$ if $u < 0$, $H[u] = 1$ if $u > 0$).

$$\underline{3 < h_0}$$

$$\text{if } 1 < h < 3\text{: } b_1 = 4v\left\{1 - \frac{3}{4}(h-1) + \frac{1}{16}(h-1)^3\right\}$$

$$\text{if } 3 < h\text{: } b_1 = 0.$$

$$\underline{h_0 < 1 \text{ (all } h < h_0)}$$

$$\Omega_N = \Omega_T = C_\infty kT[1 + 4vC_\infty].$$

$$\underline{1 < h_0 < 2}$$

$$\text{if } 0 < h < 1\text{: } \Omega_N = \Omega_T = C_\infty kT[1 + 4vC_\infty];$$

$$\text{if } 1 < h < h_0\text{: } \Omega_N = -4vC_\infty^2 kT\left[1 - \frac{3}{2}(h_0 - 1) + \frac{1}{2}(h_0 - 1)^3\right]$$

$$\Omega_T = -4vC_\infty^2 kT\left\{\left[1 - \frac{3}{2}(h_0 - 1) - \frac{1}{4}(h_0 - 1)^3\right] + \frac{3}{32}[(h_0 - 1)^3 + (2h_0 - h - 1)^3] + \frac{3}{4}(h-1)\ln\left[\frac{(h-1)}{2(h_0 - 1)}\right] - \frac{3}{4}(2h_0 - h - 1)\ln\left[\frac{2h_0 - h - 1}{2(h_0 - 1)}\right]\right\}.$$

$$\underline{2 < h_0 < 3}$$

$$\text{if } 0 < h < 1\text{: } \Omega_N = \Omega_T = C_\infty kT[1 + 4vC_\infty];$$

$$\text{if } 1 < h < 2h_0 - 3\text{: } \Omega_N = 0$$

$$\Omega_T = -4vC_\infty^2 kT\left\{-\frac{3}{8}(h-1) + \frac{3}{32}(h-1)^3 - \frac{3}{4}(h-1)\ln\left(\frac{h-1}{2}\right)\right\};$$

$$\text{if } 2h_0 - 3 < h < h_0\text{: } \Omega_N = 0$$

$$\Omega_T = -4vC_\infty^2 kT\left\{-\frac{3}{8}[(h-1) + (2h_0 - h - 1)] + \frac{3}{32}[(h-1)^3 + (2h_0 - h - 1)^3] - \frac{3}{4}(h-1)\ln\left(\frac{h-1}{2}\right) - \frac{3}{4}(2h_0 - h - 1)\ln\left(\frac{2h_0 - h - 1}{2}\right)\right\}.$$

$$\underline{3 < h_0}$$

$$\text{if } 0 < h < 1\text{: } \Omega_N = \Omega_T = C_\infty kT[1 + 4vC_\infty];$$

$$\text{if } 1 < h < 3\text{: } \Omega_N = 0$$

$$\Omega_T = -4vC_\infty^2 kT\left\{-\frac{3}{8}(h-1) + \frac{3}{32}(h-1)^3 - \frac{3}{4}(h-1)\ln\left(\frac{h-1}{2}\right)\right\};$$

$$\text{if } 3 < h\text{: } \Omega_N = \Omega_T = 0.$$

SCHEME I

solvent within any pore cross section are uniform. Furthermore, in this limit there is equilibrium at the pore ends between the solution just inside the pore and the bulk solution outside. The pore ends equilibrate with the bulk solutions to create a driving force for flow in the axial (z) direction. Note that boundary layer ("unstirred layer") effects (Pedley, 1980) are not included here; if they are significant, the term "bulk solution" as used here refers to the fluid adjacent to the membrane, and C_∞ is the solute concentration at the solution-membrane interface.

The axial gradient of solute concentration, of order $\Delta C_\infty/\ell$, is assumed sufficiently small that, on the scale of solute or pore radius, changes in distribution with respect to changes in axial position z are negligible. This is certainly an accurate assumption in the limit $\ell/\delta \to \infty$, and means that the hydrostatic stress tensor, Ω, shows the same

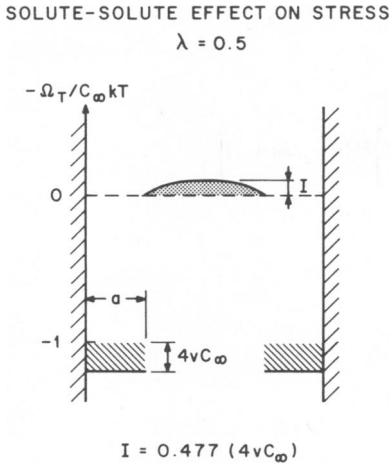

FIGURE 3 Tangential pressure profile inside slit pore, correct to $0(C_\infty^2)$.

dependence on y and C_∞ as in the equilibrium case discussed in the previous section. Note, however, that now C_∞ depends on z, where C_∞ is the solute concentration of a bulk solution that is in chemical and mechanical equilibrium with the fluid inside the pore at the cross section designated by the value of z. The dependence of C_∞ on z results in a small but important variation in Ω_T with z, which must be balanced by the fluid in the form of viscous forces resulting from flow in the z direction. If we let T be the viscous stress tensor, the differential force balance on the fluid is given by the following for this nonequilibrium situation

$$\nabla \cdot [\Omega + \mathrm{T}] - C\nabla E = 0. \tag{17}$$

The lateral components (y or r) restate mechanical equilibrium, equivalent to Eq. 7, but the z component introduces a balance between hydrostatic and viscous forces that must be solved to determine the fluid velocity.

We first consider the slit pore geometry. Dimensional considerations show that the only significant components of T are $T_{yz} = T_{zy}$. T_{zy} contributes negligibly to the y component of Eq. 17, so that

$$\frac{\partial \Omega_N}{\partial y} - C\frac{dE}{dy} = 0, \tag{18}$$

which is automatically satisfied by the equilibrium calculation of Ω, Eqs. 8–10. The z component of Eq. 17 is

$$\frac{\partial \mathrm{T}_{yz}}{\partial y} = -\frac{\partial \Omega_T}{\partial z}. \tag{19}$$

This expression can be integrated once over y, with the condition $T_{yz} = 0$ on $y = 0$, to obtain

$$T_{yz} = -\frac{\partial}{\partial z}\int_0^y \Omega_T(y')\,dy'. \tag{20}$$

To proceed further a relationship between the viscious stress T_{yz} and the z component of the mass-average fluid velocity (u_z) is needed. Assume this relationship is Newtonian. The solvent contributes to the stress through its coefficient of viscosity (η_0), while the contribution by the solute particles is designated by Σ. The "long pore" assumption allows the simple form

$$T_{yz} = \eta_0 \frac{\partial u_z}{\partial y} + \Sigma_{yz}. \tag{21}$$

The velocity field and solute viscous stress are expanded in powers of C_∞.

$$u_z = u_z^{(0)} + u_z^{(1)} + u_z^{(2)} + \ldots \tag{22a}$$

$$\Sigma_{yz} = \Sigma_{yz}^{(1)} + \Sigma_{yz}^{(2)} + \ldots \tag{22b}$$

where $u_z^{(m)}$ and $\Sigma_{yz}^{(m)}$ are $0(C_\infty^m)$. The osmotic stress is likewise an expansion in powers of C_∞ as derived in the previous section

$$\Omega_T = C_\infty kT[F_1(y) + C_\infty F_2(y) + 0(C_\infty^2)]. \tag{22c}$$

The expansion functions, $F_m(y)$, can be computed from Eqs. 8–10 for arbitrary E and U; for the specific case of HSHW interactions, F_1 and F_2 can be obtained directly from Scheme I.

The evaluation of $\Sigma_{yz}^{(1)}$, even for HSHW interactions, is difficult and represents the limiting step in this theory. The nature of this function is discussed in the Appendix. By its definition it is proportional to C_∞, and we also expect it to be proportional to $kT(dC_\infty/dz)$. Define the function $G_1(y)$ by

$$\Sigma_{yz}^{(1)}(y,z) = C_\infty kT\frac{dC_\infty}{dz}G_1(y). \tag{23}$$

The form of G_1 depends on the y dependence of $u_z^{(0)}$ as discussed in the Appendix, where it is argued that its contribution to κ_1 is quite small relative to that from Ω_T.

The osmotic velocity field is computed by substituting Eqs. 21–23 into Eq. 20 and integrating once using the "no slip" condition, $u_z = 0$, at the pore wall. The result for u_z is then averaged by integration over the pore cross section to obtain the mean velocity $\langle u_z \rangle$, which is independent of z because the pore walls are impermeable. Retaining terms up to and including $0(C_\infty)$, we have

$$\langle u_z \rangle = \frac{1}{\eta_0 \delta}\left\{\frac{1}{2}\int_0^\delta (\delta^2 - y^2)\,F_1(y)dy + \overline{C}_\infty \left[\int_0^\delta (\delta^2 - y^2)\,F_2(y)dy + \int_0^\delta yG_1(y)dy\right]\right\} kT\frac{\Delta C_\infty}{\ell}, \tag{24}$$

where $\overline{C}_\infty$ is the arithmetic mean of the two reservoir concentrations. The membrane volume flux is $\alpha \langle u_z \rangle$, where α is the pore volume fraction of the membrane. The hydraulic coefficient for a membrane with slit pores is

$$L_{po} = \frac{\alpha\delta^2}{3\eta_0\ell}. \tag{25}$$

The osmotic pressure difference, correct to $0(C_\infty)$, is computed from Eq. 11b.

$$\Delta\Pi_\infty = (1 + 2B_2\bar{C}_\infty)\,kT\Delta C_\infty$$
$$B_2 = \frac{-2\pi}{3kT}\int_0^\infty r^3\frac{dU}{dr}\exp[-U(r)/kT]dr. \tag{26}$$

The reflection coefficient is obtained by substituting Eqs. 24–26 into Eq. 1

$$\sigma = \sigma_0(1 + \kappa_1\bar{C}_\infty) \tag{27}$$

$$\sigma_0 = 3/2\,\delta^{-3}\int_0^\delta(\delta^2 - y^2)F_1(y)dy \tag{28a}$$

$$\kappa_1 = 3\sigma_0^{-1}\delta^{-3}$$
$$\cdot\left[\int_0^\delta(\delta^2 - y^2)F_2(y)dy + \int_0^\delta yG_1(y)dy\right] - 2B_2. \tag{28b}$$

Keep in mind that $0(C_\infty^2)$ terms were neglected in deriving Eq. 27. From Eqs. 8–10 and Eq. 22c one can show that

$$F_1(y) = 1 - \exp[-E(y)/kT] \tag{29}$$

for any wall potential energy, E. In principle, $F_2(y)$ can also be derived from these equations for arbitrary E and U, but the numerical work could be prohibitive in many cases.

By substituting Eq. 29 into Eq. 28a one obtains an expression for σ_0 of slit pores that has previously been derived in the $C_\infty \to 0$ limit (Anderson, 1981). For the case of HSHW interactions one obtains

$$\sigma_0 = 1/2\,\lambda^2(3 - \lambda). \tag{30}$$

The computation of κ_1 is limited by uncertainty in G_1. Estimates made in the Appendix indicate the contribution of G_1 to κ_1 is quite small. Therefore, we feel justified in neglecting this term and use the following to compute κ_1 for slit pores

$$\kappa_1 \doteq 3\sigma_0^{-1}\delta^{-3}\int_0^\delta(\delta^2 - y^2)F_2(y)dy - 2B_2. \tag{31}$$

For HSHW interactions $B_2 = 4v$ and $F_2(y)$ is obtained from the information in Scheme I. By substituting these into Eq. 31 the following expression results.

$$\lambda \geq 1: \quad \kappa_1 = 0$$
$$0.5 < \lambda < 1: \kappa_1/v = \frac{-4}{15}(h_0 - 1)^5 - \frac{82}{45}(h_0 - 1)^4$$
$$+ \frac{479}{135}(h_0 - 1)^3 + \frac{1,742}{405}(h_0 - 1)^2$$
$$- \frac{15,634}{1,215}(h_0 - 1) + \frac{2,108}{3,645}$$
$$- \frac{4,216}{3,645}\left(\frac{1}{3h_0 - 1}\right).$$
$$\lambda < 0.5: \kappa_1/v = -\frac{154}{15} + \frac{263}{15}\left(\frac{1}{3h_0 - 1}\right)$$
$$(h_0 = \lambda^{-1}). \tag{32}$$

The above relationship is plotted in Fig. 4. No concentration effect on σ is realized at $\lambda \to 1$, because no solute molecules can enter the pore in this limit; that is, the membrane is semipermeable and $\Delta\Pi_\infty$ becomes equivalent to a pressure $-\Delta P_\infty$. The greatest concentration effect occurs at $\lambda \to 0$, in which case $\kappa_1 \to -10.27v$.

The analysis for a circular cylindrical pore of radius r_0 parallels the derivation for a slit with only a few changes algebraically. The z component of Eq. 17 in cylindrical coordinates is

$$\frac{1}{r}\frac{\partial}{\partial r}(rT_{rz}) = -\frac{\partial\Omega_{zz}}{\partial z}, \tag{33}$$

which, when integrated once gives

$$T_{rz} = \frac{-\partial}{\partial z}\left[r^{-1}\int_0^r r'\Omega_{zz}(r')dr'\right]. \tag{34}$$

The assumed relationship between T_{rz} and the osmotic velocity field is the same as for the slit pore. Including terms only up to $0(C_\infty)$,

$$T_{rz} = \eta_0\frac{\partial u_z^{(0)}}{\partial r} + \left[\eta_0\frac{\partial u_z^{(1)}}{\partial r} + \Sigma_{rz}^{(1)}\right]. \tag{35}$$

As before, a function G_1^* is defined by

$$\Sigma_{rz}^{(1)} = C_\infty kT\frac{dC_\infty}{dz}G_1^*(r), \tag{36}$$

and the osmotic stress is expanded as

$$\Omega_{zz}(r) = C_\infty kT[D_1(r) + C_\infty D_2(r)]. \tag{37}$$

Following the strategy outlined for slit pores, but using

$$L_{po} = \frac{\alpha r_0^2}{8\eta_0\ell}, \tag{38}$$

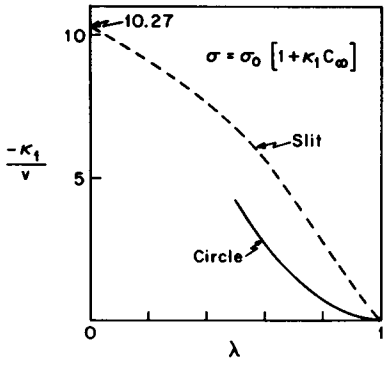

FIGURE 4 First-order coefficient (κ_1) vs. solute-to-pore size (λ). The curve for the slit pore was computed from Eq. 32.

we obtain Eq. 27 with the following expressions for the two parameters of a circular cylindrical pore

$$\sigma_0 = 4r_0^{-4}\int_0^{r_0}(r_0^2 - r^2)rD_1(r)dr \tag{39a}$$

$$\kappa_1 = 8\sigma_0^{-1}r_0^{-4}\left[\int_0^{r_0}(r_0^2 - r^2)rD_2(r)dr + \int_0^{r_0}r^2G_1^*(r)dr\right] - 2B_2. \tag{39b}$$

Closer inspection of Ω_{zz} shows that

$$D_1(r) = 1 - \exp[-E(r)/kT]. \tag{40}$$

Combining Eqs. 39a and 40 and assuming HSHW integrations yields

$$\sigma_0 = \lambda^2(4 - 4\lambda + \lambda^2), \tag{41}$$

the same result obtained earlier by neglecting solute-solute interactions (Anderson and Malone, 1974). Based on the calculations for slit pores in the Appendix, we expect the contribution of G_1^* to be small relative to the other terms and hence offer the following as a good approximation for circular cylindrical pores.

$$\kappa_1 \doteq 8\sigma_0^{-1}r_0^{-4}\int_0^{r_0}(r_0^2 - r^2)rD_2(r)dr - 2B_2. \tag{42}$$

For HSHW interactions,

$$D_2 = 4v \quad \text{if} \quad r > r_0 - a$$
$$= 4v - b_1(r) + \lim_{C_\infty \to 0}[(kTC_\infty^2)^{-1}X_{zz}^{(p)}(r)] \text{ if } r < r_0 - a. \tag{43}$$

Computations of b_1 and $X_{zz}^{(p)}$ are found elsewhere (Anderson and Brannon, 1981; Adamski, 1982). The numerical values of κ_1 computed from Eqs. 42 and 43 are listed in Table I and plotted in Fig. 4. The results are incomplete because $X_{zz}^{(p)}$ was only evaluated in the range $0.5 < \lambda < 1$. In the limit $\lambda \to 0$ the curvature of the pore wall becomes insignificant on the scale of a solute particle and κ_1 approaches $-10.27v$, the same value as for slit pores.

DISCUSSION

The quantitative validity of our numerical results for κ_1 reported in the previous section depends on several assumptions. First, the pores should be capillaries considerably longer than their width, so that the assumption of chemical and mechanical equilibrium within any pore cross section is accurate. Tight membranes, that is, those of relatively low porosity ($\lesssim$20% by volume pores) probably adhere to this requirement. Second, the calculations were performed using a hard-sphere potential function for the solute and a hard-wall potential for the pore wall. However, the basic model developed here is more general and can be applied to arbitrary solute-solute (U) and solute-pore (E) potential functions. With a computer at hand, the requisite calculations for b_1 (see Anderson and Brannon, 1981) and $X^{(p)}$ (see Eq. 13) can be made to include, say, electrostatic components in U and E. κ_1 could then be computed for charged solutes, such as proteins.

TABLE I
NUMERICAL RESULTS FOR CIRCULAR PORE

λ	$-\kappa_1/v$
0.5	4.299
0.6	2.828
0.7	1.551
0.8	0.665
0.9	0.162
1.0	0.000

Another important assumption is that the contribution of the solute toward the viscous stresses that oppose osmotic flow is small, at least at $0(C_\infty)$. We offer Eqs. 31 and 42 as good approximations for κ_1. Quantitative arguments justifying this assumption are made in the Appendix. At first thought one might conclude that the solute stress contribution, contained in G_1 and G_1^* integrals of Eqs. 28b and 39b, might be $\sim -2.5v$, because this is the $0(C_\infty)$ correction appropriate for macroscopic suspensions of rigid spheres (see Eq. A1). That the correction is an order of magnitude smaller than this, <5% of κ_1, is due to the fact that the $0(C_\infty^0)$ osmotic velocity field is uniform in the central regions of the pore and has a finite gradient only within a distance of one solute radius from the pore wall (see Fig. 5). Solute contributions to the viscous stresses are proportional to the product of velocity gradient and the local solute concentration. Because the concentration of solute particles, by volume fraction, is very small near the pore wall, there is little interaction between them and the velocity gradient, and hence the net contribution of $\Sigma_{yz}^{(1)}$ is small relative to the $0(C_\infty)$ correction to the gradient of osmotic stress.

Fig. 4 shows that the magnitude of κ_1 increases as λ decreases for each pore geometry. This result is perhaps not too surprising when one considers the λ equals 1 limit. In this case no solute molecules can enter the pore, and hence $\Omega_T = -P_0(z)$ throughout the entire pore cross

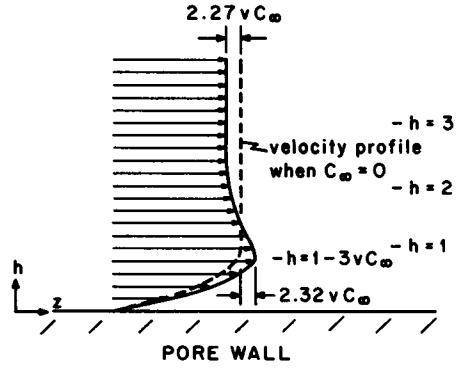

FIGURE 5 Dimensionless osmotic velocity, $[U_z/(a^2kT/2\eta_0)(dC_\infty/dz)]$, vs. position from pore wall (h = distance/a) for a large slit pore ($\lambda < 1/3$). When $C_\infty = 0$ and $h \geq 1$, the dimensionless velocity equals 1. Solute/pore wall interactions are assumed to be of the HSHW type.

section. Because $P_0 = -\Pi_\infty$, there is no concentration effect ($\kappa_1 = 0$) and the osmotic flow has the same strength as if a pressure difference $\Delta P_\infty = -\Delta\Pi_\infty$ were applied. This limiting result is true to any order of C_∞ considered. On the other hand, at the $\lambda = 0$ limit the solute molecules can crowd around each other at the pore wall, without being screened by the wall as much as when it is curved ($\lambda > 0$), so that solute-solute interactions are greatest here. Note that as $\lambda \to 0$ for any shape pore, $\kappa_1 \to -10.27v$ since the pore wall appears flat on a local scale (~0 [a]), and thus the slit result is valid for all geometries in this limit.

The different results for κ_1 for the two geometries can be explained using the above discussion. At given λ for slit and circle, the circular pore provides more shielding between solute molecules, which reduces the concentration effect. One would thus expect the magnitude of κ_1 to be greater for the slit pore than for the circular pore, as is obvious from Fig. 4. However, a comparison of Eqs. 30 and 41 indicates that, at the same λ, the value of σ_0 is greater for the circular pore. Given the general trend that $-\kappa_1$ increases as λ decreases, one might expect a correlation between κ_1 and σ_0 that is less sensitive to pore geometry. Such a graph is shown in Fig. 6, and remarkably, the calculations for slit and circle appear to lie on one line. By performing a one-parameter, least-squares fit to the calculated points in Fig. 6, omitting the $\lambda = 0$ point, we obtained the following

$$\kappa_1 = -9.66(\sigma_0 - 1). \tag{44}$$

This result is very nice in that it seems to be independent of pore geometry (a slit and circle are opposite extremes of simple pore cross-sectional geometries).

The direct use of κ_1 in Eq. 2, with $0(C_\infty^2)$ terms neglected, is of limited quantitative usefulness. Before suggesting a way to get around this problem, we consider whether or not

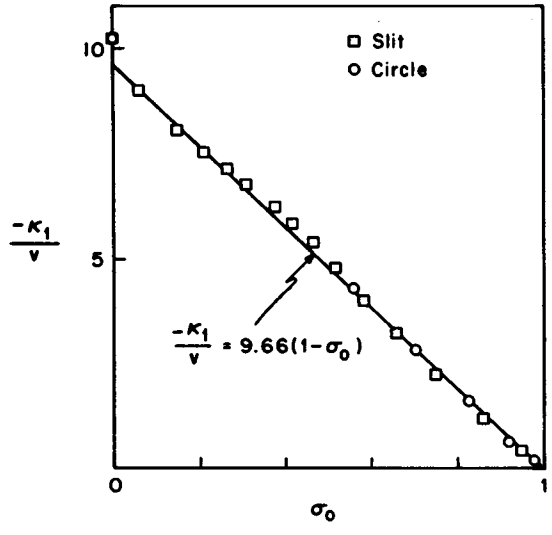

FIGURE 6 The straight line was fit by a least-square criterion. σ_0 is computed from Eq. 30 for the slit and Eq. 41 for the circle, while the values for κ_1 were taken from Fig. 4.

the next term is a function only of $\bar{C}_\infty^2$, or if it actually depends on both reservoir concentrations ($C_\infty[0]$ and $C_\infty[\ell]$). If $0(C_\infty^3)$ terms are included in Ω_T and Π_∞, Eqs. 24 and 26 adopt the forms

$$\langle u_z \rangle = \eta_0^{-1}\left\{A_1 + A_2\bar{C}_\infty + A_3\bar{C}_\infty^2\left[1 - \frac{C_\infty(0)C_\infty(\ell)}{4\bar{C}_\infty^2}\right]\right\}\frac{\Delta C_\infty}{\ell} \tag{45}$$

$$\Delta\Pi_\infty = kT\left\{1 + 2B_2\bar{C}_\infty^2\left[1 - \frac{C_\infty(0)C_\infty(\ell)}{4\bar{C}_\infty^2}\right]\right\}\Delta C_\infty, \tag{46}$$

where the A_n are constants obtained by integrating certain functions of y over the pore cross section. If we now use these expressions to compute σ, the $0(C_\infty^2)$ term will include both $\bar{C}_\infty^2$ and the ratio $C_\infty(0)C_\infty(\ell)/4\bar{C}_\infty^2$. The latter term is negligible if one reservoir concentration is much lower than the other. Assuming this is the case, we can write

$$\sigma = \sigma_0[1 + \kappa_1\bar{C}_\infty + \kappa_2\bar{C}_\infty^2], \tag{47}$$

with negligible error.

The determination of κ_2, even for HSHW interactions in a slit pore, presents a formidable computational challenge. Although b_2 (the $0[C_\infty^2]$ coefficient of Eq. 4) can be estimated (Anderson and Brannon, 1981) the calculation of $\chi^{(p)}$ by Eq. 13 requires $\rho^{(2)}$ correct to $0(C_\infty^3)$, which, to our knowledge, has not been done. Even if Kirkwood's superposition approximation is used for $\rho^{(2)}$ to get this next term, the extra numerical integrations required to obtain $\chi^{(p)}$ would be quite time consuming. A more appealing approach is to rewrite Eq. 27 as

$$\sigma \approx \frac{\sigma_0}{1 - \kappa_1\bar{C}_\infty}. \tag{48}$$

The $0(\bar{C}_\infty)$ expansion of this expression gives $\kappa_1\bar{C}_\infty$, as required, while the next term, $\kappa_1^2\bar{C}_\infty^2$ is positive. We expect the coefficient, κ_2, is also positive, because values of σ less than zero must be avoided even as $\bar{C}_\infty$ increases. Thus, Eq. 48 may offer a reasonable approximation for the dependence of σ on $\bar{C}_\infty$ at moderate solute concentrations.

Data for osmotic reflection coefficient vs. solute concentration were reported by Friedman and Meyer (1981) for aqueous sucrose solutions across Cuprophan membranes. These authors defined the reflection coefficient (σ_v) by

$$J_v = -\sigma_v L_p\, kT\, \Delta C_\infty, \tag{49}$$

which differs from our definition in Eq. 1. If concentration effects on L_p are neglected, our coefficient (σ) is related to theirs by

$$\sigma = \sigma_v kT\frac{\Delta C_\infty}{\Delta\Pi_\infty} = \sigma_v kT\left[\left(\frac{\partial\Pi_\infty}{\partial C_\infty}\right) + \frac{1}{2}\left(\frac{\partial^2\Pi_\infty}{\partial C_\infty^2}\right)\Delta C_\infty + 0(\Delta C_\infty^2)\right]^{-1}, \tag{50}$$

with the partial derivatives taken at constant temperature. The $0(\Delta C_\infty)$ term is negligible for their experimental

conditions. The relationship between Π_∞ and C_∞ can be determined from the thermodynamic coefficients plotted in their Fig. 3 ($\bar{\nu}_s$ is the volume fraction of sucrose as determined by density vs. concentration data, $\Gamma = [(\partial \ell n \gamma / \partial \ell n C_\infty)]_{T,P}$, where γ is the activity coefficient)

$$\frac{\partial \Pi_\infty}{\partial C_\infty} = kT \frac{(1 + \Gamma)}{(1 - \bar{\nu}_s)}. \tag{51}$$

If the surcrose molecules are modeled as hard spheres having no long range forces, the equation of state is (McQuarrie, 1976)

$$\frac{\partial \Pi_\infty}{\partial C_\infty} = kT \frac{(1 + 4\varphi_\infty + 4\varphi_\infty^2)}{(1 - \varphi_\infty)^4}, \tag{52}$$

Where $\varphi_\infty = \upsilon C_\infty$, and υ is the equivalent hard-sphere volume of one molecule. If Eqs. 51 and 52 are combined with the values for Γ and $\bar{\nu}_s$ as plotted by Friedman and Meyer (1981), the equivalent hard-sphere volume is obtained using a least-square error criterion, $\upsilon = 1.53 \times 10^{-22}$ cm^3, or an equivalent hard-sphere radius of 3.3 Å.

The values of σ that we computed from Friedman and Meyer's data (1981) for σ_v and Eq. 50 are listed in Table II. It appears that σ is nearly constant, or even increases slightly as C_∞ increases, in contradiction with our theoretical predictions. This disagreement does not mean our theory is invalid; rather, it could mean that a hard-sphere model for sucrose is incorrect. In support of this contention, consider that the ratio $\bar{\nu}_s/C_\infty$ equals 3.53×10^{-22} cm^3, which is quite a bit larger than the equivalent hard-sphere volume. This volume per molecule yields a hydrated sucrose molecular radius equal to 4.4 Å, which is relatively close to the Stokes-Einstein radius 4.7 Å (obtained from the infinite-dilution diffusion coefficient). The small value of the equivalent hard-sphere radius (3.3 Å) implies that there exists a substantial attractive component to the pair potential (U) between two sucrose molecules. Further evidence for this attraction can be found in the fact that the mutual diffusion coefficient of sucrose decreases as C_∞ increases (Gosting and Morris, 1949), although the hard-sphere theory predicts the opposite behavior (Batchelor, 1976). With regard to our theoretical model, the existence of an attractive component to the pair potential would increase κ_1 (make it less negative), and hence σ would change very little or perhaps even increase as C_∞ increases. Thus, we conclude that although the data for sucrose by Friedman and Meyer (1981) are very important in their own right, they do not represent a good test of our theoretical model. Note that the behavior of sucrose is characteristic of most simple sugars.

TABLE II
REFLECTION COEFFICIENT* VS. $\bar{C}_\infty$ FOR AQUEOUS SUCROSE SOLUTIONS ACROSS CUPROPHAN MEMBRANES

$\bar{C}_\infty$	σ
moles/liter	
0.30	0.24
0.45	0.25
0.70	0.26
0.90	0.24

*σ, as defined by Eq. 1, was computed from data by Friedman and Meyer (1981).

The paper by Schultz et al. (1979) illustrates how concentration effects might influence the interpretation of osmotic flow data. These authors measured osmotic flow rates resulting from concentration differences of various molecular weight Dextrans across Nuclepore membranes.[2] The dependence of Π_∞ on C_∞ was also measured, so the experimental values of J_v and $\Delta\Pi_\infty$ were used in Eq. 1 to obtain σ. As Fig. 7 shows, the experimental determinations are significantly below the σ_0 curve computed for hard spheres. Schultz et al. (1979) concluded that Dextrans, because of their deformability, exhibit a smaller reflection coefficient than a rigid sphere having the same Stokes-Einstein radius. We suggest that concentration effects could have contributed to some of the disagreement.

To interpret the results of Schultz et al. (1979) in terms of concentration effects, we take the solute volume to be $(4/3)\pi a^3$, where a is the Stokes-Einstein radius. (In the case of Dextrans, the hard-sphere radius computed from the second osmotic virial coefficient agrees with the hydrodynamic radius calculated from intrinsinc viscosity [Brannon and Anderson, 1982].) In their experiments, the mean volume fraction of solute, υC_∞, was in the range 0.1–0.2. Because the pores of the membranes were circular, we use Eq. 41 for σ_0 and predict σ from Eqs. 44 and 48. The filled symbols in Fig. 7 are these estimates. The predictions are generally much lower than the σ_0 curve, indicating a substantial concentration effect. Although the theory cannot account for all differences between the data and the σ_0 curve of Fig. 7, it does show that concentration effects probably contributed to a significant fraction of these differences.

Areekul (1969) measured reflection coefficients of neutral and negatively charged Dextrans in a perfused rabbit ear membrane. He observed substantial reductions in σ as the Dextran concentration increased over the range 0.5–5.0% by weight. It is interesting that Areekul interpreted these reductions in σ to imply that the membrane became more leaky (i.e., the number of leaky channels increased) as the Dextran concentration increased. Our model is consistent with these experimental observations without postulating any changes in membrane structure.

Our definition of σ in Eq. 1 is slightly different than given in some texts. Specifically, some individuals use L_p in the denominator instead of L_{po}, where L_p should be considered a function of C_∞. We chose L_{po} to avoid having to solve another problem, namely that of the $0(C_\infty)$ solute effect on

[2]Actually, the authors used an extrapolation procedure to determine the pressure difference required to halt the flow.

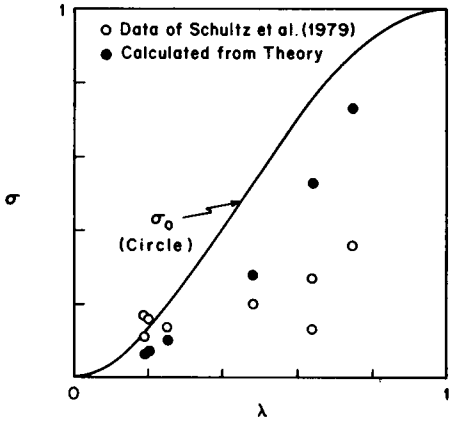

FIGURE 7 Data for Dextrans in Nuclepore membranes. The theoretical calculations were performed using Eqs. 41, 44, and 48.

the hydraulic coefficient of a membrane. The use of L_{po} also has practical advantage in that the hydraulic coefficient need only be determined with pure solvent and hence the experimentor does not have to worry about plugging the membrane pores with solute when he applies mechanical pressure differences to make the determination. In the experiments of Schultz et al. (1979) and Friedman and Meyer (1981) σ was defined using L_p instead of L_{po}, so that a small adjustment would have to be made ($L_p \leq L_{po}$) to these measurements to give σ as defined in Eq. 1 here.

In summary, we have proposed a model for the concentration dependence of osmotic reflection coefficient based on pore structure, solute-solute interactions, and viscous flow. The important results are Eqs. 31 and 42. Although the theory is formally only correct to $0(C_\infty)$, it can probably be extended to higher concentrations using Eq. 48. The calculations presented here are valid for solute-membrane systems experiencing only HSHW interactions, but the theory is more general. Besides any possible equantitative usefulness of the analysis, it deserves notice because it predicts some concentration dependence of σ even when the proper concentration dependence of $\Delta\Pi_\infty$ is accounted for. Our message is that experimental determinations of σ should be extrapolated to $C_\infty = 0$ if the results are to be interpreted in terms of pore or solute structure.

APPENDIX

Solute Contribution to Viscous Stresses

$\Sigma^{(1)}_{yz}$ represents the $0(C_\infty)$ effect by the solute on the fluid's ability to resist deformation caused by gradients in the osmotic stress. This effect arises because the solute particles are rigid. Because the contribution is $0(C_\infty)$, its calculation must involve the first-order expression for solute distribution, $C_\infty \exp(-E/kT)$, and the zero-order osmotic velocity field, $u_z(0)$. According to the mathematical expansion developed in our theory, solute-solute hydrodynamic interactions do not figure in the computation of κ_1, but must be considered if κ_2 is calculated.

According to Faxen's law (Batchelor and Green, 1972; Brenner and Haber, 1983), the stress produced by rigid spheres of radius a, volume $v = (4/3)\pi a^3$, and concentration C is given by

$$\Sigma^{(1)} = 5vC\eta_0\left[e^{(0)} + \frac{a^2}{10}\nabla^2 e^{(0)}\right], \tag{A1}$$

where η_0 is the solvent viscosity and $e^{(0)}$ the rate of strain dyadic of the solvent, if the particles were not there,

$$e^{(0)} = \frac{1}{2}[\nabla u^{(0)} + \nabla u^{(0)^T}]. \tag{A2}$$

Eq. A1 applies to solutions that are dilute ($vC \ll 1$) and unbounded. Although the latter requirement is not met in our system, we shall neglect any effect that the pore wall might have on $\Sigma^{(1)}$.

We consider a slit pore first. The $0(C_\infty^0)$ osmotic velocity field is determined by integrating Eq. 20 just once using Eqs. 22 and setting $u_z^{(0)} = 0$ at the pore wall.

$$u_z^{(0)} = \frac{kT}{\eta_0}\frac{dC_\infty}{dz}\frac{(a^2)}{2} \quad \text{if} \quad y < \delta - a$$

$$= \frac{kT}{\eta_0}\frac{dC_\infty}{dz}(\delta - y)\left[a - \frac{1}{2}(\delta - y)\right] \quad \text{if} \quad \delta - a < y < \delta. \tag{A3}$$

The relevant component of $e^{(0)}$ is

$$e^{(0)}_{yz} = 0 \quad \text{if} \quad y < \delta - a$$

$$= -\frac{kT}{\eta_0}\frac{dC_\infty}{dz}[y - (\delta - a)] \quad \text{if} \quad \delta - a < y < \delta. \tag{A4}$$

The concentration field, correct to $0(C_\infty)$, is

$$C = C_\infty \exp[-E(y)/kT]$$
$$= C_\infty \text{ if } y < \delta - a \tag{A5}$$
$$= 0 \text{ if } \delta - a < y < \delta$$

After substituting Eqs. A4 and A5 into Eq. A1, we obtain G_1 as defined by Eq. 23

$$G_1 = -\frac{v}{2}[1 - F_h(y^*)]\left[5y^* F_h(y^*) + \frac{a^2}{2}F_d(y^*)\right], \tag{A6}$$

where $y^* = y - (\delta - a)$, and F_h and F_d are the Heaviside step function and the Dirac delta function, respectively. Substitution of this expression into Eq. 28b produces a correction ($\Delta\kappa_1$) due to hydrodynamic effects of the solute particles

$$\Delta\kappa_1 = -\frac{3(1-\lambda)}{4(3-\lambda)}v. \tag{A7}$$

In Table III we list some values of κ_1, as computed from Eq. 31 (or Eq. 32), and $\Delta\kappa_1$, from Eq. A7. The correction, $\Delta\kappa_1$, is generally only 2% of the magnitude of κ_1, and in our opinion, negligible. Thus, Eq. 31 is an excellent approximation, and there is no need to include solute effects on the viscous stresses arising from the osmotic flow. The reason why solute

TABLE III
VALUES OF HYDRODYNAMIC CORRECTION

λ	(κ_1/v)*	$(\Delta\kappa_1/v)$‡
0	−10.27	−0.25
0.33	− 8.08	−0.19
0.50	− 6.76	−0.15
0.67	− 4.79	−0.11
1	0	0

*Computed from Eq. 32.
‡Computed from Eq. A7.

molecules do not significantly contribute to the viscous stress is found in their distribution; solute molecules are constrained to the central region of the pore ($y < \delta - a$), where $e_{yz}^{(0)}$ is zero, and only the $\nabla^2 e^{(0)}$ part of $\Sigma^{(1)}$ is nonzero as the pore wall is approached.

A similar analysis can be made for circular pores. For hard-sphere interactions, the rate of strain of the $0(C_\infty^0)$ osmotic flow is

$$e_{rz}^{(0)} = 0 \quad \text{if} \quad r < r_0 - a$$
$$= -\frac{kT}{4\eta_0}\left[r - \frac{(r_0 - a)^2}{r}\right] \quad \text{if} \quad r_0 - a < r < r_0. \qquad \text{(A8)}$$

From this expression and Eq. A1, one can obtain G_1^* as defined in Eq. 36. If this is substituted into Eq. 39b, there results

$$\Delta\kappa_1 = -\frac{(1-\lambda)^2}{(4 - 4\lambda + \lambda^2)}\,\upsilon. \qquad \text{(A9)}$$

Numerical examples show that $\Delta\kappa_1$ is 3% or less the magnitude of κ_1 determined by Eq. 42, so we conclude that the solute effect on the viscous stress is negligible.

We appreciate the financial support of the National Science Foundation. Discussions with Professors H. Brenner and E. Glandt were very helpful. John L. Anderson thanks the John Simmon Guggenheim Foundation and the Massachusetts Institute of Technology for their support during his sabbatical leave.

Received for publication 26 July 82 and in final form 4 April 1983.

REFERENCES

Adamski, R. P. 1982. The effect of bulk solute concentrations on the osmotic reflection coefficient. Master thesis, Carnegie-Mellon University, Pittsburgh, PA.

Anderson, J. L. 1981. Configurational effect on the reflection coefficient for rigid solutes in capillary pores. *J. Theor. Biol.* 90:405–426.

Anderson, J. L., and D. M. Malone. 1974. Mechanism of osmotic flow in porous membranes. *Biophys. J.* 14:957–982.

Anderson, J. L., and J. H. Brannon. 1981. Concentration dependence of the distribution coefficient for macromolecules in porous media. *J. Polym. Sci. Polym. Physics Ed.* 19:405–421.

Anderson, J. L. 1982. Concentration effects on distribution of macromolecules in small pores. *Adv. Colloid Interface Sci.* 16:391–401.

Areekul, S. 1969. Reflection coefficients of neutral and sulphate-substituted dextran molecules in the isolated perfused rabbit ear. *Acta Soc. Med. Upsal.* 74:129–138.

Batchelor, G. K., and J. T. Green. 1972. The determination of the bulk stress in a suspension of spherical particles to order C^2. *J. Fluid Mech.* 56:401–419.

Batchelor, G. K. 1976. Brownian diffusion of particles with hydrodynamic interaction. *J. Fluid Mech.* 74:1–18.

Brannon, J. H., and J. L. Anderson. 1982. Concentration effects on partitioning of dextrans and serum albumin in porous glass. *J. Polym. Sci. Polym. Physics Ed.* 20:857–865.

Brenner, H., and S. Haber. 1983. Symbolic operator representation of generalized Faxén relations. *Physicochem. Hydrodynamics.* In press.

Curry, F. E., J. C. Mason, and C. C. Michel. 1976. Osmotic reflexion coefficients of capillary walls to low molecular weight hydrophilic solutes measured in single perfused capillaries of the frog mesentery, *J. Physiol. (Lond.).* 261:319–336.

Friedman, M. H., and R. A. Meyer. 1981. Transport across homoporous and heteroporous membranes in nonideal, nondilute solutions. I. Inequality of reflecting coefficients or volume flow and solute flow. *Biophys. J.* 34:535–545.

Giddings, J. C., E. Kucera, C. P. Russell, and M. N. Meyers. 1968. Statistical theory for the equilibrium distribution of rigid molecules in inert porous networks. Exclusion chromatography. *J. Phys. Chem.* 72:4397–4409.

Glandt, E. D. 1980. Density distribution of hard-spherical molecules inside small pores of various shapes. *J. Colloid Interface Sci.* 77:512–524.

Gosting, L. J., and M. S. Morris. 1949. Diffusion studies on dilute aqueous sucrose solutions at 1 and 25° with the Gouy interference method, *J. Am. Chem. Soc.* 71:1998–2005.

Hill, T. L. 1960. An Introduction to Statistical Mechanics, McGraw-Hill, New York, Chapter 19.

Irving, J. H., and J. G. Kirkwood. 1950. The statistical mechanical theory of transport processes. IV. The equations of hydrodynamics. *J. Chem. Phys.* 18:817–824.

Levitt, D. G. 1975. General continuum analysis of transport through pores. I. Proof of Onsager's reciprocitry postulate for uniform pore. *Biophys. J.* 15:533–563.

Massaldi, H. A., and C. H. Borzi. 1982. Non-ideal phenomena in osmotic flow through selective membranes. *J. Membr. Sci.* 12:87–96.

Mauro, A. 1960. Some properties of ionic and non-ionic semipermeable membranes. *Circulation.* 21:845–854.

McQuarrie, D. A. 1976. Statistical Mechanics. Harper and Row, New York, 279.

Pedley, T. J. 1980. The interaction between stirring and osmosis, part 1. *J. Fluid Mech.* 101:843–861.

Rudin, A. 1971. Concentration effects in gel permeation chromatography. *J. Polym. Sci. Part A-1.* 9:2587–2591.

Satterfield, C. N., C. K. Colton, B. D. Turckheim, and T. M. Copeland. 1978. Effect of concentration on partitioning of polystyrene within finely porous glass. *AIChE. J.* 24:937–944.

Schultz, J. S., R. Valentine, and C. Y. Choi. 1979. Reflection coefficients of homopore membranes: effect of molecular size and configuration. *J. Gen. Physiol.* 73:49–60.

Staverman, A. J. 1951. The theory of measurement of osmotic pressure. *Rec. Trav. Chim. Pays-Bas Belg.* 70:344-364.